Prostate cancer localization using multi-parametric MRI and a maximum likelihood classification algorithm

Sharon Clarke[1], Bruce Daniel[2], Jesse McKenney[3], Manojkumar Saranathan[2], Brian Hargreaves[2], James Brooks[4], Harachan Gill[4], Mark Gonzalgo[4], Benjamin Chung[4], Emine Saritas[5], Ajit Shankaranarayanan[6], and Graham Sommer[2]

[1]Diagnostic Radiology, Dalhousie University, Halifax, Nova Scotia, Canada, [2]Diagnostic Radiology, Stanford University, Stanford, California, United States, [3]Anatomic Pathology, Cleveland Clinic, Cleveland, Ohio, United States, [4]Urology, Stanford University, Stanford, California, United States, [5]Bioengineering, University of California Berkeley, Berkeley, California, United States, [6]GE Healthcare, Menlo Park, California, United States

Purpose: Prostate cancer is the second most frequently diagnosed cancer and the sixth leading cause of cancer death among men worldwide (1). Multi-parametric MRI of the prostate gland utilizing T2-weighted, diffusion weighted, and contrast-enhanced imaging has shown potential to identify clinically significant prostate tumors for MR-guided biopsy or focal therapy (2,3). The purpose of this study was to use a semi-automated classification of multi-parametric MR images to identify prostate cancer, and to perform a quantitative comparison of the segmentation results with histopathology.

MRI Methods: Our institution's ethics review board approved this prospective study. Between January and June 2012, twenty-two men scheduled for prostatectomy for biopsy-proven prostate adenocarcinoma were recruited for pre-operative MRI of the prostate gland. After informed consent was obtained, the subjects were imaged on a 3T GE MR750 system (GE Healthcare, Waukesha, WI) using a 32-channel RF coil. Pulse sequences used included respiratory-triggered axial T2 FSE with fat saturation (TE=92 ms, ETL 14, FOV 22 cm, matrix 416 x 224, slice spacing 4 mm), reduced FOV diffusion-weighted EPI (4), (b values 100, 200, 400, 800 and 1600 s/mm^2 with NEX= 2, 4, 8, 12, and 12, respectively, TR/TE 4000/67 ms, FOV 20 x 10 cm, matrix 128 x 64, slice thickness 5 mm) and dynamic contrast-enhanced (DCE) MRI with DISCO (5), which is a dual-echo SPGR acquisition employing Dixon water-fat separation, a pseudo-random variable density k-space segmentation, and a view sharing reconstruction. A keyhole imaging technique was incorporated into the DCE MRI acquisition and reconstruction, resulting in a temporal resolution of less than 3 seconds (TR/TE 4.3/1.9ms, FOV 30 cm, matrix 256 x 256, 2 x 2 acceleration, slice thickness 1.6 mm).

Analysis: Outlines of the prostate gland, including zonal boundaries, were drawn on the axial T2-weighted FSE images by a radiologist and saved without the associated MR image. A single expert genitourinary pathologist, who was blinded to the MRI results, examined each prostatectomy specimen and manually drew regions of adenocarcinoma on the prostate gland outlines to create a "tumor map". The Gleason score of each tumor region was also recorded.

An apparent diffusion coefficient (ADC) map was calculated using the b = 100, 200, 400, 800 s/mm^2 images. The MR images of the prostate gland were segmented into tumor and non-tumor regions using the maximum likelihood classification algorithm with ENVI software (Boulder, CO). Input for the classifier included the T2-weighted FSE, ADC map, early arterial phase contrast-enhanced images, and the b=1600 s/mm^2 EPI diffusion-weighted images. Small regions of interest representing both tumor and benign prostate tissue on 4 different subjects were used to train the classifier. The training regions represented <15% of the total number of pixels to be classified in the training data set. The trained classifier was then used to classify the remaining >85% of the pixels in the training set, as well as images from subjects not included in the training set. The accuracy of the segmented images was assessed on a pixel-by-pixel basis by comparison with the pathologist's tumor maps.

Results: Representative ADC map, T2-weighted FSE, reduced FOV diffusion-weighted EPI, and arterial phase images of the prostate gland are shown in figure 1. Small regions of interest from these images were included in the training data set. The result of the maximum likelihood classification is also shown, alongside the corresponding tumor map. The classifier accuracy in the case shown in figure 1 was 77% (Kappa = 0.55). In the training data set, the overall accuracy of the maximum likelihood algorithm was 85%. Figure 2 illustrates the results of the maximum likelihood classifier in a different subject whose images were not included in the training data set. The classifier accuracy for the case shown in figure 2 was 92% (Kappa = 0.77). In general, classification accuracy increased with higher Gleason scores.

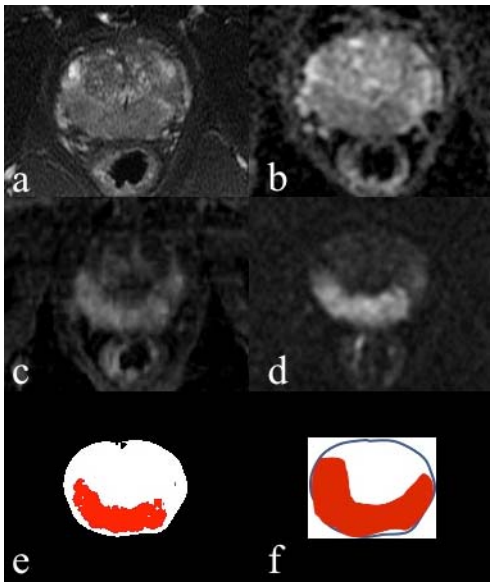

Figure 1: representative MR images and segmentation results. Shown are T2 weighted FSE (a), ADC map (b), arterial phase (c), diffusion with b=1600 s/mm^2 (d), maximum likelihood classification (e) and tumor "map" (f) where red represents tumor (Gleason 4+3 and 3+4).

Figure 2: Maximum likelihood result compared with the tumor map in a subject whose images were not used to train the classifier. Red represents tumor (Gleason score 4+4)

Conclusion: Segmentation of multi-contrast MR images of the prostate gland using a supervised classification algorithm correlates well with histopathology. These results show promise for identification of clinically relevant prostate cancer for either MR-guided biopsy or focal therapy.

References: 1. Jemal et al., *Ca Cancer J Clin* 2011;61:69–90; **2**. Turkbey et al., *Curr Opin Urol* 2012, 22:310 – 315; **3**. Moradi et al., *Journal Of Magnetic Resonance Imaging* 2012 35:1403–1413; **4.** Saritas, EU et al., *Magn Reson Med* 2008 Aug;60(2):468-73; **4.** Saranathan et al., *J. Magn. Reson. Imaging* 2012;35:1484–1492.